Sirt3 Regulates Metabolic Flexibility of Skeletal Muscle Through Reversible Enzymatic Deacetylation

Enxuan Jing,[1] Brian T. O'Neill,[1] Matthew J. Rardin,[2] André Kleinridders,[1] Olga R. Ilkeyeva,[3] Siegfried Ussar,[1] James R. Bain,[3] Kevin Y. Lee,[1] Eric M. Verdin,[4,5] Christopher B. Newgard,[3] Bradford W. Gibson,[2] and C. Ronald Kahn[1]

Sirt3 is an NAD^+-dependent deacetylase that regulates mitochondrial function by targeting metabolic enzymes and proteins. In fasting mice, Sirt3 expression is decreased in skeletal muscle resulting in increased mitochondrial protein acetylation. Deletion of Sirt3 led to impaired glucose oxidation in muscle, which was associated with decreased pyruvate dehydrogenase (PDH) activity, accumulation of pyruvate and lactate metabolites, and an inability of insulin to suppress fatty acid oxidation. Antibody-based acetyl-peptide enrichment and mass spectrometry of mitochondrial lysates from WT and Sirt3 KO skeletal muscle revealed that a major target of Sirt3 deacetylation is the E1α subunit of PDH (PDH E1α). Sirt3 knockout in vivo and Sirt3 knockdown in myoblasts in vitro induced hyperacetylation of the PDH E1α subunit, altering its phosphorylation leading to suppressed PDH enzymatic activity. The inhibition of PDH activity resulting from reduced levels of Sirt3 induces a switch of skeletal muscle substrate utilization from carbohydrate oxidation toward lactate production and fatty acid utilization even in the fed state, contributing to a loss of metabolic flexibility. Thus, Sirt3 plays an important role in skeletal muscle mitochondrial substrate choice and metabolic flexibility in part by regulating PDH function through deacetylation. ***Diabetes*** **62:3404–3417, 2013**

Skeletal muscle is the major oxidative tissue in mammals. Metabolic flexibility, i.e., the ability to switch between glucose and lipid oxidation, in muscle is essential to maintain normal energy metabolism and physiology. In the fed state, the main fuel source in muscle is insulin-induced glucose metabolism (1,2); during fasting, muscle switches its fuel utilization from glucose to lipid oxidation (3). Insulin resistance, type 2 diabetes, and obesity are strongly associated with impaired skeletal muscle substrate metabolism including decreased fasting lipid oxidation, impaired postprandial glucose oxidation, and reduced capacity for lipid oxidation during exercise (4,5). Thus, the flexibility and capacity of substrate metabolism are compromised in muscle in these states.

From the [1]Section on Integrative Physiology and Metabolism, Joslin Diabetes Center, Harvard Medical School, Boston, Massachusetts; the [2]Buck Institute for Research on Aging, Novato, California; the [3]Department of Medicine, Duke University Medical Center, Durham, North Carolina; the [4]Gladstone Institute of Virology and Immunology, San Francisco, California; and the [5]Department of Medicine, University of California, San Francisco, San Francisco, California.

Corresponding author: C. Ronald Kahn, c.ronald.kahn@joslin.harvard.edu.

Received 27 November 2012 and accepted 26 June 2013.

DOI: 10.2337/db12-1650

This article contains Supplementary Data online at http://diabetes.diabetesjournals.org/lookup/suppl/doi:10.2337/db12-1650/-/DC1.

E.J. and B.T.O. contributed equally to this study.

Recent reports have shown that mitochondrial dysfunction is a major contributor to the development of insulin resistance and diabetes (6,7). Transcription factors regulating mitochondrial function and biogenesis, such as peroxisome proliferator–activated receptor (PPAR)γ coactivator-1α, nuclear respiratory factor-1, and PPARα play critical roles in insulin sensitivity, glucose metabolism, and lipid metabolism in muscle (8–11). Mutations of key metabolic enzymes and subunits of the electron transporter chain can also lead to mitochondrial dysfunction and various degrees of myopathy and neuropathology. Among these, pyruvate dehydrogenase (PDH) complex deficiency due to mutations of the E1α subunit gene (PDHA1) that encodes the catalytic subunit of PDH is a genetic cause of mitochondrial dysfunction and inherited neurodegenerative disease in humans, implicating this subunit's critical role in metabolism (12,13).

The PDH complex catalyzes the rate-limiting step in aerobic carbohydrate metabolism and mediates the efficient conversion of pyruvate from glycolysis to energy in cells. The activity of this multienzyme complex is regulated, at least in part, by reversible phosphorylation of serine residues of the E1α subunit through PDH kinases (PDHKs) and PDH phosphatases whose enzymatic functions are regulated by cellular nutrient cues (14). Phosphorylation by PDHKs inhibits the E1α subunit, decreasing PDH activity; accordingly, inhibition of PDHKs is a potential therapeutic target for diabetes (15). Nutrient deprivation, such as starvation or diabetes, leads to increased NAD^+-to-NADH ratio and increases PDHK expression and activity, thereby inhibiting PDH in muscle; this is reversible with refeeding or insulin treatment (16). Besides phosphorylation, recent studies suggest that reversible acetylation/deacetylation may also regulate PDH catalytic subunit E1α (PDH E1α) function (17–19), although the pathways controlling this process have not been fully elucidated.

In recent years, NAD^+-dependent deacetylases called sirtuins (Sirt) have been shown to play important roles in metabolism (20,21). Among seven members of this protein family, Sirt3 is identified as the major mitochondrial deacetylase (22,23). Several recent studies have shown that Sirt3 regulates lipid metabolism, energy production, and stress response in different tissues through its deacetylase activity (24–26). In muscle, Sirt3 expression is regulated by nutrient signals and contractile activity and impacts downstream signaling events through AMP-activated protein kinase activation and PPARγ coactivator-1α expression (27,28). Sirt3 was implicated in the development of metabolic disease in humans when a commonly identified polymorphism that decreases Sirt3 activity was found to be associated with the development of metabolic syndrome (29). We previously demonstrated that skeletal muscle Sirt3 expression is downregulated in rodent models of diabetes

and upregulated by caloric restriction and that decreased Sirt3 expression induces oxidative stress and impairs insulin signaling in muscle (30). Sirt3 also regulates levels of reactive oxygen species (ROS) through deacetylation of SOD2 (26,31). In the current study, using a combination of proteomic, metabolomic, and functional approaches, we demonstrate that skeletal muscle Sirt3 regulates substrate metabolism by targeting mitochondrial PDH E1α subunit and PDH enzyme activity and thus optimizes the complex and intricate switch of substrate utilization between glucose and lipid oxidation and substrate flexibility.

RESEARCH DESIGN AND METHODS

Animal studies were performed according to protocols approved by the Institutional Animal Care and Use Committee. Male C57Bl/6 mice or *Sirt3*$^{-/-}$ and wild-type (WT) littermate controls backcrossed onto a C57Bl/6 background and maintained on a standard chow diet were used. Fed mice were allowed ad libitum access to food and killed at 9:00 A.M. For fasting studies, mice were transferred to a new cage without food for 24 h and then killed or refed for 4 or 16 h prior to sacrifice.

Insulin signaling in muscle strips. Extensor digitorum longus (EDL) or hemidiaphragms were dissected and incubated for 30 min in Krebs-Henseleit buffer (KHB) at 37°C and then transferred to KHB with or without 1 or 10 mU/mL insulin for 10 min. Muscle strips were blotted and snap frozen in liquid nitrogen.

Glycolysis, glycogen synthesis, glucose oxidation, and palmitate oxidation in muscle strips. Glycolysis, glycogen synthesis, glucose oxidation, and palmitate oxidation were measured in isolated muscle strips as previously described with the following modifications (32). Briefly, hemidiaphragms and EDL muscles were dissected and incubated for 30 min in KHB gassed with 95% O_2 and 5% CO_2. Muscle strips were transferred to gassed KHB containing 5 mmol/L glucose and 0.2 mmol/L palmitate bound to 3% fatty acid–free BSA, with or without 1 mU/mL insulin, and with radiolabeled tracers. For glycolysis, glycogen synthesis, and glucose oxidation, incubation buffer contained 20 μCi/mmol [U-^{14}C]glucose and 80 μCi/mmol [5-^{3}H]glucose, and muscles were incubated for 1 h with shaking at 37°C. Reactions were terminated by removal of the tissue from the incubation medium, followed by injection of 0.2 mL hyamine hydroxide into the center wells and 0.1 mL 70% (w/v) $HClO_4$ into 1 mL of the contents of the flask. The rate of glucose oxidation was determined from the production of $^{14}CO_2$. Glycogen was purified by digestion of tissue in 1 mol/L NaOH and then precipitation in 66% ethanol with 100 mg unlabeled glycogen to determine the amount of glycogen synthesized from [U-^{14}C]glucose and [5-^{3}H]glucose incorporation. $^{3}H_2O$ formation was measured by separating $^{3}H_2O$ from 0.5 mL incubation buffer containing [5-^{3}H]glucose on Poly-Prep Columns AG 1-X8-731-6212 (Bio-Rad) pretreated with 1 mol/L NaOH and then 0.3 mol/L Boric acid. The rate of glycolysis was determined from the difference between the rate of $^{3}H_2O$ formed and the rate of substrate recycling determined from the difference between the rates of glycogen synthesis from [U-^{14}C]glucose and [5-^{3}H]glucose.

Cell culture maintenance. C2C12 cells (American Type Culture Collection, Manassas, VA) were maintained in high-glucose Dulbecco's modified Eagle's medium (DMEM) (Invitrogen) containing 10% FBS (Gemini Bioproducts) unless otherwise indicated. *Sirt3* short hairpin RNA (shRNA) and short hairpin green fluorescent protein (shGFP) control lentiviral constructs were purchased from Open Biosystems (Huntsville, AL). Stable Sirt3 knockdown and shGFP control cell lines were generated by viral transduction of C2C12 myoblasts and selection with puromycin. Wild-type PDH E1α cDNA lentiviral construct (Genecopeia) was used for site-directed mutagenesis (Stratagene) to generate K336Q and K336R mutations and further sequenced. WT, K336Q, and K336R overexpressing stable C2C12 cell lines were generated.

Proteomic analysis of acetylated skeletal muscle mitochondrial peptides. Mitochondria were isolated from hindlimb muscle of WT and SIRT3 KO mice as previously described (33) with the following adaptations: Muscle was homogenized with teflon-pestle in Medium 1 with deacetylase inhibitors (250 mmol/L sucrose, 1 mmol/L EDTA, and 10 mmol/L Tris-HCl, pH 7.4; protease and phosphatase inhibitors [PIs] [Sigma]; 10 mmol/L nicotinamide; and 1 μmol/L trichostatin A). Mitochondria were enriched by differential centrifugation and purified by centrifugation at 59,800*g* on 5–25% (w/v) linear Ficoll (Sigma) gradients. Purified mitochondria were lysed in radioimmunoprecipitation assay buffer containing protease, phosphatase, and deacetylase inhibitors. Approximately 1 mg total mitochondrial protein was digested with trypsin, and an acetylated peptide fraction was prepared using a combination of anti-AcK antibodies from ImmuneChem (cat. no. ICP0380-100) and Cell Signaling (cat. no. 9441) as previously described (34). Peptides were analyzed by reversed-phase nano-high-performance liquid chromatography electrospray tandem mass spectrometry (HPLC-ESI-MS/MS) on a QSTAR Elite mass spectrometer. The resulting MS/MS datasets were analyzed using Mascot 2.3.2 (Matrix Sciences) and Protein Pilot 4.1 (AB Sciex, Foster City, CA) searched against the mouse SwissProt database (SwissProt 2011_04). Peptide scores outside of the 5% local false discovery rate were excluded. Skyline MS1 Filtering (34) was used to quantify changes in the MS1 ion abundances among acetylated peptides between WT and KO mice.

PDH activity assay. PDH activity was measured using two methods. The first used the Mitosciences Pyruvate Dehydrogenase Enzyme Activity Microplate Assay Kit (Abcam) in which PDH complexes from isolated mitochondria or cellular lysates are immunocaptured on a microplate. A reaction medium containing pyruvate and NAD^+ is then added. The readout is the rate of production of NADH, which is coupled to a dye whose formation is monitored on a spectrophotometric plate reader, and activity is calculated from the rate of change in optical density at 410 nm. For in vivo experiments, muscle mitochondria were isolated as previously described (35), and equal amounts of mitochondrial protein were loaded into the immunocapture plate. For in vitro experiments, confluent myoblasts were treated as specified in the manufacturer's protocol. For specified experiments, PI cocktails 2 and 3 (Sigma) or 20 mmol/L dichloroacetate (DCA) was added to detergent-soluble fraction and buffer 1 prior to microplate incubation. Activity was normalized to protein content of the detergent-soluble fraction. For Western blots of extracts from PDH activity experiments, an aliquot of detergent soluble extracts was incubated at room temperature for 3 h to mimic microplate conditions and blotted using phospho-specific PDH E1α antibodies.

PDH activity was also measured in whole muscle homogenates based on the evolution of $^{14}CO_2$ from ^{14}C-labeled pyruvate (36). Briefly, gastrocnemius muscle from randomly fed mice was snap frozen until use. Muscle homogenates (50 mg wet weight/mL) were incubated for 15 min at 37°C with either *1*) "inactivation" buffer containing 50 mmol/L NaF and 8 mmol/L ATP to prevent dephosphorylation of the PDH complex with or without the addition of deacetylase inhibitors (1 mmol/L nicotinamide and 1 μmol/L trichostatin A) or *2*) "activation" buffer containing 1 μg recombinant PDH phosphatase 1 (Abcam), 5 mmol/L DCA, 9 mmol/L $MgCl_2$, and 0.1 mmol/L $CaCl_2$ with or without deacetylase inhibitors. Activity was then measured in 20 μL homogenates diluted in reaction buffer for 10 min and terminated with 20% trichloroacetate and 30 mmol/L pyruvate as described in the protocol. Evolved $^{14}CO_2$ was collected in suspended center wells containing 1 mol/L hyamine hydroxide in methanol and counted in 4 mL Cytoscint scintillation fluid. Activity of homogenates treated with inactivating solution was termed "PDHa," as this likely represents the native activation of PDH in muscle. Activity of homogenates treated with activating solution was termed "PDHt," representing total activity of PDH present in muscle.

ATP and glycogen measurement. ATP levels were measured by an enzymatic coupled assay as previously described (37). Briefly, metabolites were isolated from pulverized muscle in 6% perchloric acid and neutralized with KOH and imidazole, and then ATP was measured as the change in optical density at 340 nm after addition of glucose, $NADP^+$, glucose-6-phosphate dehydrogenase, and hexokinase. Glycogen content was measured as previously described (38).

Immunoprecipitation and Western analysis. Powdered muscle tissue, isolated muscle mitochondria, or confluent myoblasts were homogenized in radioimmunoprecipitation assay buffer (Millipore) with protease and PIs (Sigma) and deacetylase inhibitors (10 mmol/L nicotinamide/1 μmol/L trichostatin A). Lysates were subjected to SDS-PAGE and blotted using PDH E1α, PDHK4, LCAD, glyceraldehyde-3-phosphate dehydrogenase, insulin receptor β (Santa Cruz), phospho-IR/IGFR, phospho-Akt, phospho-ERK, Akt, extracellular signal–related kinase (ERK), VDAC, Sirt3, (Cell Signaling), or acetyl-lysine (Immunechem or Cell Signaling) antibodies. For immunoprecipitation assays, mitochondria were isolated in the presence of protease and deacetylase inhibitors as previously described (35), resuspended in IP lysis buffer (Pierce), and immunoprecipitated with anti–acetyl-lysine (AcK) agarose beads (Immunechem) with streptavidin beads (Pierce) as a control.

Oxygen consumption rate and extracellular acidification rate assays. Cellular oxygen consumption rate (OCR) was measured using a Seahorse Bioscience XF24 flux analyzer. Cells were seeded at 30,000 cells/well 24 h prior to the analysis in low-glucose (100 mg/dL) DMEM containing 10% FBS. Each experimental condition was analyzed using four to six biological replicates. For OCR experiments using palmitate, KHB buffer (pH 7.4) was added to each well and measurements were performed every 3 min with 2 min intermeasurement mixing. BSA-conjugated palmitate (final concentration 200 μmol/L) and etomoxir (final concentration 50 μmol/L) were injected sequentially. For extracellular acidification rate (ECAR) experiments with glucose as a substrate, sodium carbonate and glucose/pyruvate-free DMEM was used. Glucose and 2-deoxyglucose were injected sequentially to give final concentrations of 25 mmol/L.

Metabolomic assays for skeletal muscle amino acids, organic acids, and acylcarnitines. Amino acids, acylcarnitines, and organic acids were analyzed using stable isotope dilution techniques. Amino acids and acylcarnitine measurements were made by flow injection MS/MS using sample preparation methods described previously (39,40). The data were acquired using a Micromass Quattro MicroTM system equipped with a model 2777 autosampler, a model 1525 HPLC solvent delivery system, and a data system controlled by MassLynx 4.1 operating system (Waters, Millford, MA). Organic acids were quantified using methods described previously with Trace Ultra GC coupled to a Trace DSQ MS operating under Xcalibur 1.4 (Thermo Fisher Scientific, Austin, TX) (41).

Statistical analyses. All data are means ± SEM. Student *t* test was performed for comparison of two groups or ANOVA was performed for comparison of three or more groups to determine significance.

RESULTS

Sirt3 expression and mitochondrial acetylation is regulated by fasting. Quantitative real-time PCR using quadriceps (Quad), EDL, and soleus muscles from 8-week-old male WT C57Bl/6 mice revealed that 24 h of fasting suppressed Sirt3 mRNA expression in hindlimb muscles (Fig. 1*A*). All of these reductions returned to close to fed levels by 16 h of refeeding and the EDL muscle showed some recovery as early as 4 h after refeeding (Supplementary Fig. 1*A*). Western blotting analysis confirmed a parallel ~50% decrease of Sirt3 protein level in soleus and gastrocnemius muscle from fasted mice, which increased after refeeding to near-normal levels, as we have previously described in quadriceps (30) (Fig. 1*B*). There was some variability in the recovery of Sirt3 levels from experiment to experiment, but a decrease in Sirt3 levels in the fasted state was observed in all muscle groups tested (Supplementary Fig. 1*A* and *C*). In the fasted state, levels of expression also varied, with muscle fiber type being highest in red soleus and lower in white EDL muscle.

Western analysis of isolated mitochondria from skeletal muscle using an antibody against AcK revealed a general increase of mitochondrial protein acetylation after 24 h of fasting, coinciding with decreased Sirt3 levels. We observed a specific increase in acetylation of bands at 97, 72, and 47 kDa (Fig. 1*C*). The lower hyperacetylated band was in the migration position of PDH catalytic subunit E1α. We immunoprecipitated muscle mitochondrial lysates isolated from either fed or fasted mice using anti-AcK antibody and subjected the immunoprecipitates to Western blotting analysis with anti–PDH E1α antibody. The abundance of the PDH E1α protein from the immunoprecipitates represents its acetylation status. This analysis confirmed hyperacetylation of PDH E1α in fasted skeletal muscle (Fig. 1*D*).

Posttranslational modifications known to suppress PDH activity include PDH kinase–mediated phosphorylation targeting three serine residues of PDH E1α (S232, S293, and S300) (42). We tested serine phosphorylation of PDH E1α in muscle mitochondria using phospho-specific antibodies and found that S232 and S300 phosphorylation was increased during fasting coincident with the PDH E1α hyperacetylation (Fig. 1*D*). The changes in PDH E1α acetylation/phosphorylation after fasting were not explained by changes in PDH E1α total protein levels (Fig. 1*D*).

Sirt3 deletion induces a shift in substrate utilization away from glucose oxidation and increases PDH E1α phosphorylation suppressing PDH activity. We hypothesized that Sirt3 has its most prominent role in metabolic regulation in the fed state, when it is present at highest levels. To test this hypothesis, we assessed glucose and palmitate oxidation, as well as glycolysis and glycogen synthesis, in isolated muscle strips from fed WT and Sirt3 KO mice to fully characterize muscle substrate metabolism in the absence of Sirt3. Glucose oxidation in EDL muscles (composed primarily of glycolytic fibers) in the presence of 5 mmol/L glucose, 0.2 mmol/L palmitate, and 1 mU/mL insulin was significantly decreased in Sirt3 KO mice compared with controls (Fig. 2*A*). However, glycogen synthesis rates responded normally to insulin, and glycolytic rates were unchanged in Sirt3 KO, suggesting that glucose uptake was normal but that the end products of glycolysis were not fully oxidized in Sirt3 KO muscle generating lactate. Palmitate oxidation rate was quite low in EDL muscle and was unchanged between KO and WT. To determine whether these changes were due to insulin resistance, as we have observed in older 24-week animals (30), we measured insulin signaling in muscle strips from 8- to 16-week-old Sirt3 KO mice and controls. Interestingly, in this ex vivo experiment in EDL strips from younger mice in the fed or fasted state, we found no difference in insulin signaling between Sirt3 KO mice and controls (Fig. 2*B*). In hemidiaphragms (composed of more oxidative fibers) palmitate oxidation was increased in the presence of insulin, and glucose oxidation was not significantly changed in Sirt3 KO but tended to decrease (Fig. 2*C*). Again, there was no change in insulin signaling, glycolysis, or glycogen synthesis rates in hemidiaphragms from Sirt3 KO compared with WT controls (Supplementary Fig. 2*A* and *B*). These changes in substrate metabolism did not affect total glycogen content or ATP levels in tissues isolated in the fed or fasted states, and AMP-activated protein kinase phosphorylation was decreased in Sirt3 KO muscle upon fasting as previously described (Supplementary Fig. 2*D* and *E*) (27).

The decreased glucose oxidation rate in the insulin-stimulated state in muscle samples from Sirt3 KO mice indicated a potential regulatory role for Sirt3 on mitochondrial glucose oxidation. Since PDH E1α function can be regulated by phosphorylation on three serine residues (42), we assessed phosphorylation of PDH E1α in WT and Sirt3 KO skeletal muscle to determine whether deletion of Sirt3 mimics the effect of fasting on posttranslational modification of PDH E1α. Knockout of Sirt3 resulted in an increase in the phosphorylation of PDH E1α on S300 and tended to increase S232 (but not S293) in muscle of fed mice (Fig. 2*D* and Supplementary Fig. 2*F*), mimicking the increased phospho–PDH E1α observed in fasted WT mice. As observed in fasting, increased PDH E1α acetylation and phosphorylation in Sirt3 KO occurred without changes in the total level of PDH E1α or PDHK4 in either the fed or the fasted state (Fig. 2*D* and *F*).

Posttranslational modifications like phosphorylation of PDH E1α are known to have effects on PDH enzymatic activity (14,43); thus, we investigated whether the increased acetylation and phosphorylation of PDH E1α related to Sirt3 deletion would change catalytic activity of the PDH enzyme complex. Indeed, PDH activity measured by the immunocapture assay (see RESEARCH DESIGN AND METHODS) was significantly reduced in Sirt3 KO mitochondrial lysates compared with WT. Quantification of the slopes of the linear regressions demonstrated a >70% inhibition of PDH activity in KO mice (Fig. 2*E*). To further elucidate the possible regulatory role of acetylation on PDH activity, we determined active and total PDH activity in muscle homogenates from fed Sirt3 KO and WT mice as well as fasted C57Bl/6 mice by measurement of $^{14}CO_2$ production from ^{14}C-labeled pyruvate in the presence or absence of deacetylase inhibitors (see RESEARCH DESIGN AND METHODS). As in the mitochondrial isolates, PDHa activity

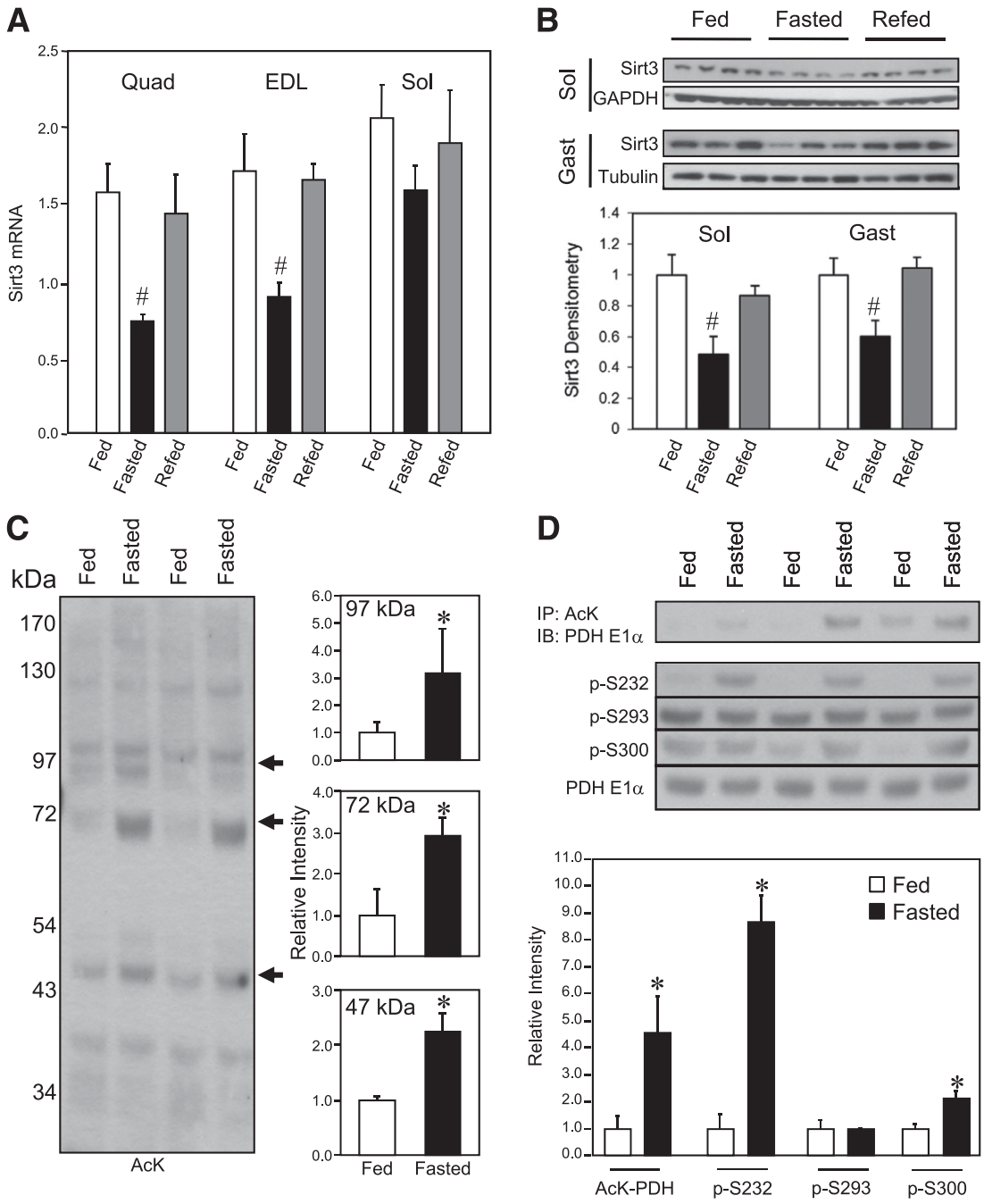

FIG. 1. Skeletal muscle Sirt3 expression and mitochondrial protein acetylation are regulated by fasting. Wild-type 8-week-old male C57Bl/6 mice were fed ad libitum, fasted for 24 h, or fasted and then refed for 16 h. After each treatment, RNA and protein were extracted and analyzed by real-time quantitative PCR (*A*) or Western blotting (*B*) for assessment of Sirt3 expression in quadriceps (Quad), EDL, soleus (Sol), and gastrocnemius (Gast) muscle groups (n = 3–5, #P < 0.05 vs. fed, ANOVA). *C*: Mixed hindlimb muscles (gastrocnemius and soleus) were collected from mice in the fed or fasted state. Muscle mitochondria were isolated in the presence of protease and deacetylase inhibitors as described in RESEARCH DESIGN AND METHODS. Mitochondrial protein lysates from each animal were subjected to SDS-PAGE and Western blotting using an antibody against AcK. The intensity of specified bands was quantified with ImageJ software (n = 3, *P < 0.05, Student t test). *D*: PDH E1α acetylation in muscle of fed or fasted mice was measured by immunoprecipitation (IP) of mitochondrial lysates using anti-AcK antibody. Immunoprecipitates were subjected to Western blotting analysis (IB) using anti–PDH E1α antibody. The same muscle mitochondrial lysates were directly subjected to SDS-PAGE electrophoresis and Western blotting using antibodies against phosphorylated serine sites p-232, p-293, and p-300 of the PDH E1α subunit and total protein of PDH E1α. Autoradiography of Western blots was quantified with ImageJ software (n = 3, *P < 0.05, Student t test). GAPDH, glyceraldehyde-3-phosphate dehydrogenase.

was significantly decreased in Sirt3 KO muscle to the level of fasted C57Bl/6 mice (Fig. 2*G*) without any changes in total PDH (Supplementary Fig. 2*C*). Remarkably, incubation of the muscle homogenates in the absence of deacetylase inhibitors, which likely allows other deacetylases outside the mitochondria but present in the tissue homogenate to act on PDH, partially restored PDH activity from Sirt3 KO mice. Since inhibition of PDH activity in fasting muscle has profound effects on substrate metabolism, the observed reduction of PDH activity induced by Sirt3 deletion demonstrates that Sirt3 is an important regulator of the metabolic changes in fed skeletal muscle.

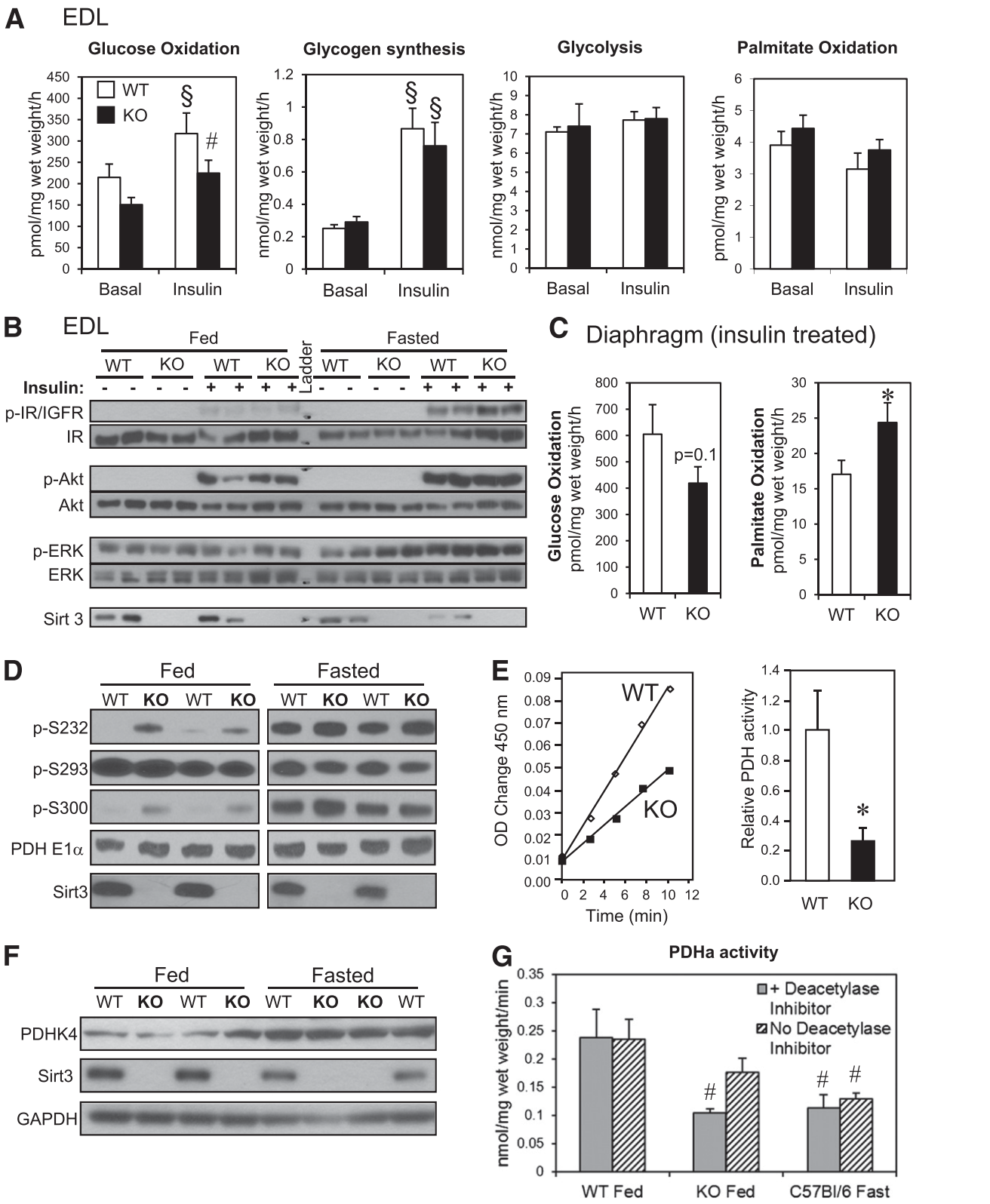

FIG. 2. Sirt3 deletion induces synergistic switch from glucose oxidation toward fatty acid oxidation and suppresses PDH activity by inducing PDH E1α hyperacetylation and hyperphosphorylation in fed Sirt3 KO skeletal muscle. *A*: Basal and insulin-stimulated (1 mU/mL) glucose oxidation, glycogen synthesis, glycolysis, and palmitate oxidation were measured in EDL muscles isolated from randomly fed 8- to 16-week-old WT and Sirt3 KO mice (n = 9; §P < 0.05 vs. basal, #P < 0.05 vs. WT, ANOVA). *B*: Basal and insulin-stimulated (10 mU/mL) phosphorylation of insulin/IGF-1 receptor, Akt, and ERK in tissue lysates of EDL muscles from fed and fasted 8- to 16-week-old WT and Sirt3 KO mice. *C*: Insulin-stimulated (1 mU/mL) glucose and palmitate oxidation were measured as described in RESEARCH DESIGN AND METHODS in diaphragms isolated from randomly fed 8- to 16-week-old WT and Sirt3 KO mice (n = 9; *P < 0.05, Student t test). *D*: Mitochondrial lysates were subjected to Western blot analysis using antibodies against p-232, p-293, and p-300 serine phosphorylation sites on PDH E1α, total PDH E1α, and Sirt3 (densitometry in Supplementary Fig. 2*F*). *E*: PDH activity was measured in 20 mg mitochondrial lysate from hindlimb of fed WT and Sirt3 KO mice using a PDH activity microplate kit as described in RESEARCH DESIGN AND METHODS. The PDH activities were calculated by linear regression of the steady-state kinetics and quantified (n = 4–5,

PDH E1α subunit is a Sirt3 substrate. Using anti-AcK antibody to detect protein acetylation, we observed that Sirt3 KO muscle mitochondria displayed an elevation in acetylation similar to that seen in fasted WT mice (Fig. 3*A*), supporting the idea that Sirt3 is the primary mitochondrial deacetylase and consistent with our previous report in Sirt3 KO fed mice (23,30). To identify the potential Sirt3 targets in skeletal muscle during fasting (when Sirt3 levels are low) and in Sirt3 KO muscle, we performed a global acetyl-proteomic analysis (34). To this end, acetylated peptides were enriched from trypsinized mitochondrial protein lysates of WT and Sirt3 KO muscle using AcK antibody immunoprecipitation and subjected to mass spectrometry analysis. A total of 549 acetylated peptides were identified in the combined WT and KO muscle mitochondria. Among these, 299 acetylated peptides were present in both WT and KO samples, only 49 of which were detected exclusively in WT, whereas 201 acetylated peptides were exclusive to the Sirt3 KO, indicating increased acetylation induced by Sirt3 deletion (Fig. 3*B*). These 549 acetylated peptides corresponded to a total of 147 acetylated proteins, indicating that there were multiple acetylation sites for each protein (Fig. 3*B*). Our analysis revealed several lysine acetylation sites on PDH E1α (Fig. 3*C*). Among the peptides showing significantly increased acetylation in Sirt3 KO muscle mitochondria was one peptide representing acetylated lysine 336 (K336) of PDH E1α (Supplementary Fig. 3*A*). Quantitation of the MS1 precursor signals of this peptide between the four WT and four KO mice showed a threefold increase in acetylation at K336 in the Sirt3 KO animals (Fig. 3*D*), indicating that K336 is a substrate of Sirt3.

To confirm that Sirt3 directly acetylates PDH, we immunoprecipitated WT and Sirt3 KO muscle mitochondrial lysates from both fed and fasted mice using anti-AcK antibody and subjected the immunoprecipitates to Western blotting analysis with anti-PDH E1α antibody. This revealed that PDH E1α acetylation was increased significantly in Sirt3 KO muscle mitochondria (Fig. 3*E*), and this was specific, as no enrichment was observed using streptavidin beads as a control (Supplementary Fig. 3).

Sirt3 deletion in skeletal muscle induces an altered metabolic profile. To fully assess the metabolic effects of PDH E1α inhibition in Sirt3 KO skeletal muscle, we performed targeted gas chromatography/mass spectrometry and MS/MS metabolomic analysis on samples of skeletal muscle from fed WT and Sirt3 KO mice. We found significantly elevated levels of lactate, pyruvate, and α-ketoglutarate (α-KG) in Sirt3 KO skeletal muscle (Fig. 4*A*). The increase in lactate and pyruvate in Sirt3 KO muscles is consistent with suppression of PDH activity and decreased carbohydrate oxidation. We also observed a significant decrease in levels of acylcarnitines measured in Sirt3 KO muscle, suggestive of increased fatty acid use (Fig. 4*B*). Additionally, amino acids levels were decreased in Sirt3 KO muscle (Fig. 4*C*). Taken together, these metabolomic data indicate that Sirt3 deletion induces a metabolic derangement in skeletal muscle in which impaired PDH activity suppresses glucose oxidation and enhances lipid and amino acid catabolism.

Knockdown of Sirt3 in C2C12 myoblasts decreases PDH activity. To further elucidate the role of Sirt3 in PDH function, we determined PDH E1α acetylation and enzyme activity in C2C12 myoblasts in which Sirt3 was knocked down using shRNA (shSirt3). This resulted in a >90% decrease in Sirt3 protein by Western analysis (Fig. 5*A*, *C*, and *D*). Immunoprecipitation of mitochondrial lysates from shGFP control and shSirt3 myoblasts using anti-AcK antibody revealed significantly increased acetylated PDH E1α in knockdown cells (Fig. 5*A*). The increased acetylation of PDH E1α in vitro was associated with a 27% decrease in PDH activity in shSirt3 myoblasts measured by microplate immunocapture of PDH (Fig. 5*B*). However, in contrast to results in skeletal muscle in vivo from Sirt3 KO mice, shSirt3 myoblasts showed decreased phosphorylation at both S232 and S300 sites (Fig. 5*C* and *D*), suggesting that PDH E1α acetylation may inhibit PDH activity independent of phosphorylation.

Previous bioenergetic profiling using Seahorse XF flux analyzer with glucose and pyruvate as substrates showed that shSirt3 myoblasts had significantly lower uncoupled respiration (30). Since changes in the metabolomic profile suggested a switch in substrate utilization in Sirt3 KO muscles, we measured glucose and fatty acid oxidation occurred in a cell autonomous manner using shSirt3 knockdown myoblasts. Basal rates of lactate production, as indicated by ECAR, were similar in control and shSirt3 myoblasts. When given glucose as substrate, shSirt3 cells displayed a greater increase in ECAR compared with control (Fig. 5*E*). The area under the curve (AUC) quantification of ECAR was significantly higher in shSirt3 after glucose stimulation (Fig. 5*F*). As previously reported, OCRs were lower in shSirt3 myoblasts (Supplementary Fig. 4*A* and *B*) (30). OCR in the presence of 200 μmol/L palmitate was significantly higher in shSirt3 cells, and this was inhibited by addition of etomoxir, indicating higher rates of fatty acid β-oxidation in shSirt3 compared with control cells. AUC calculation after palmitate showed a ~35% increase in OCR in shSirt3 (Fig. 5*G* and *H*). Together, these data demonstrate that decreased Sirt3 expression induces a switch in muscle substrate utilization from glucose to fatty acid oxidation to compensate for decreased carbohydrate oxidation caused by inhibition of PDH activity.

Overexpression of K336Q or K336R mutants of PDH E1α decreases phosphorylation at S232 and S300 but does not affect PDH activity or substrate metabolism. To determine whether acetylation at lysine 336 of PDH E1α was sufficient to affect PDH activity, we created C2C12 myoblast cell lines with stable overexpression of WT PDH E1α or with either a K336Q or a K336R mutation. In some molecules, the lysine (K) to glutamine (Q) mutation can mimic the acetylated state, while the K to arginine (R) prevents acetylation and mimics the deacetylated state. Both K336Q and the K336R mutations caused a reduction in phosphorylation of S232 and S300 compared with overexpression of WT PDH E1α (Fig. 6*A* and *B*), indicating an important role of lysine 336 in control of serine phosphorylation. To dissect the effect of phosphorylation status versus K336 mutation on PDH activity, we determined PDH activity in the presence of PIs to promote phosphorylation

***$P < 0.05$, Student t test). *F*: Western blot analysis was performed on tissue lysates from gastrocnemius muscle from fed and fasted WT and Sirt3 KO for PDHK4, Sirt3, and glyceraldehyde-3-phosphate dehydrogenase. *G*: Native PDH activity (PDHa) was measured in gastrocnemius muscle homogenate from WT fed, Sirt3 KO fed, and fasted C57Bl/6 mice by collection of $^{14}CO_2$ release from ^{14}C-pyruvate. Prior to PDH assay, aliquots of homogenates were incubated in the presence of 50 mmol/L NaF with or without deacetylase inhibitors (1 mmol/L nicotinamide and 1 mol/L trichostatin A) as described in RESEARCH DESIGN AND METHODS (n = 6–7; #$P < 0.05$ vs. WT plus deacetylase inhibitors, ANOVA). OD, optical density.**

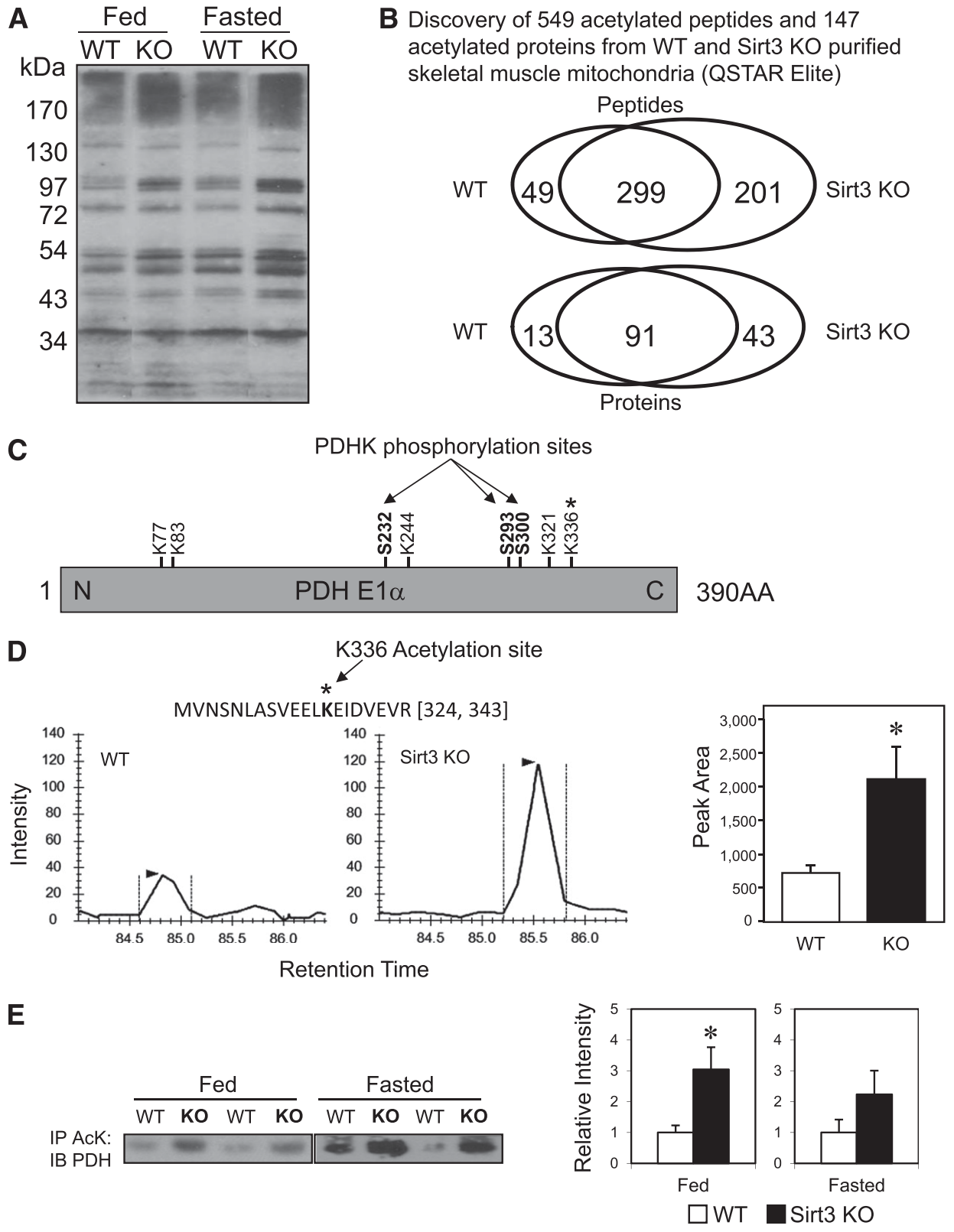

FIG. 3. Discovery of PDH E1α subunit as a target of Sirt3 in skeletal muscle. *A*: Muscle mitochondrial protein lysates from WT and Sirt3 KO mice in either the fed or fasted state were subjected to Western blotting analysis using anti-AcK antibody. *B*: Proteomic analysis using anti-AcK antibody–based acetylated peptide enrichment and mass spectrometry discovered a total of 549 acetylated peptides present in WT and Sirt3 KO skeletal muscle mitochondria. These peptides represented a total of 147 proteins. Venn diagrams show overlapping and distinctive patterns of distribution of acetylated peptides and proteins between WT and Sirt3 KO skeletal muscle. *C*: Schematic diagram of lysine acetylation sites and previously reported serine phosphorylation sites on PDH E1α. *D*: A representative MS1 chromatogram of the triply charged precursor peak at m/z 772.7303^{3+} (324-MVNSNLASVEELacKEIDVEVR-343) of PDH E1α was highly increased in Sirt3 KO skeletal muscle mitochondria compared with WT (n = 4; P < 0.05, Student t test). *E*: Skeletal muscle mitochondrial lysates from WT and Sirt3 KO mice in both fed and fasted states were immunoprecipitated (IP) with AcK antibody–bound beads. Immunoprecipitates of the mitochondrial lysate were subjected to Western blotting (IB) using an anti–PDH E1α antibody. Densitometry of either fed or fasted animals was calculated (n = 4; *P < 0.05, Student t test).

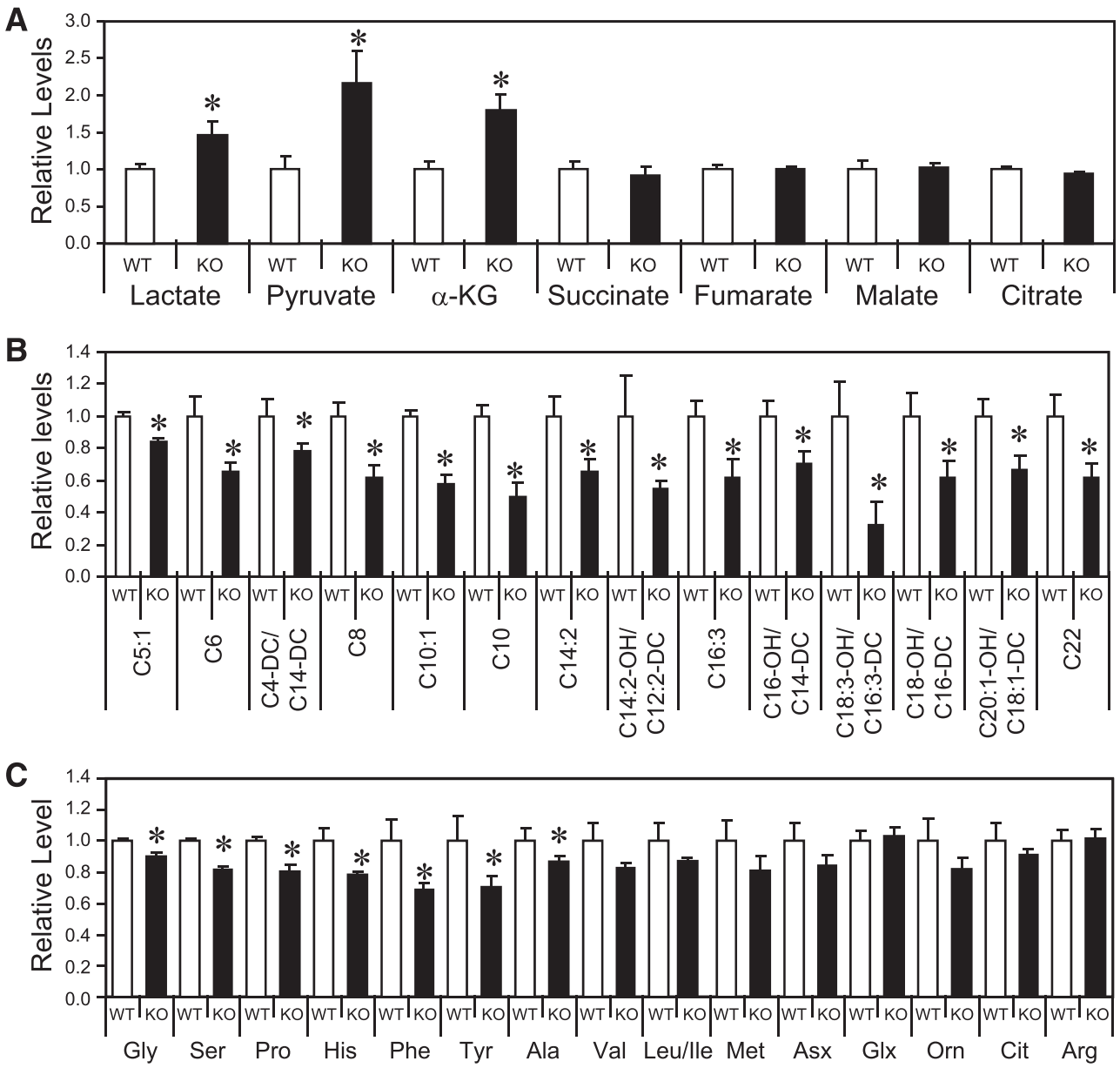

FIG. 4. Sirt3 deletion induces a substrate switch and derangement of metabolites in skeletal muscle. Quadriceps muscles from fed male WT and Sirt3 KO mice were collected and subjected to metabolomic analysis as described in RESEARCH DESIGN AND METHODS. Relative levels of organic acids and Kreb cycle intermediates are shown in *A*, levels of acylcarnitines in *B*, and amino acid levels in *C* (n = 4–5; *P < 0.05, Student t test). Asx, asparagine and aspartic acid; Cit, citrulline; Glx, glutamine and glutamic acid; Orn, ornithine.

or DCA, a PDH kinase specific inhibitor, to decrease phosphorylation of PDH E1α. PDH activity was unchanged in myoblasts harboring either of the K336Q or K336R mutations compared with WT controls (Fig. 6*C*) with or without addition of PI to preserve S293 and S300 phosphorylation or addition of DCA to maximally dephosphorylate PDH E1α (Fig. 6*D*).

To assess whether K336Q or K336R mutations could recapitulate the substrate switch observed in shSirt3 cells, we analyzed glucose-induced ECAR in WT, K336Q, or K336R myoblasts. No significant differences in glucose-stimulated ECAR were observed in the K336Q or K336R mutant cells compared with control (Fig. 6*E* and *F*). Thus, altering the ability of K336 to undergo acetylation did modify phosphorylation of PDH E1α but could not fully recapitulate the effects of decreased Sirt3 expression on PDH complex activity and substrate metabolism.

DISCUSSION

Mitochondrial sirtuins are uniquely positioned to regulate energy metabolism via protein deacetylation. Although Sirt3, Sirt4, and Sirt5 have all been localized to mitochondria, previous reports have shown that only Sirt3 deletion induces mitochondrial protein hyperacetylation, suggesting that Sirt3 is the major mitochondrial protein deacetylase (23). Indeed, recent studies have shown that altered Sirt3 expression can have effects on lipid metabolism, ROS production, oxidative stress response, and cell survival (25,26,30,44,45).

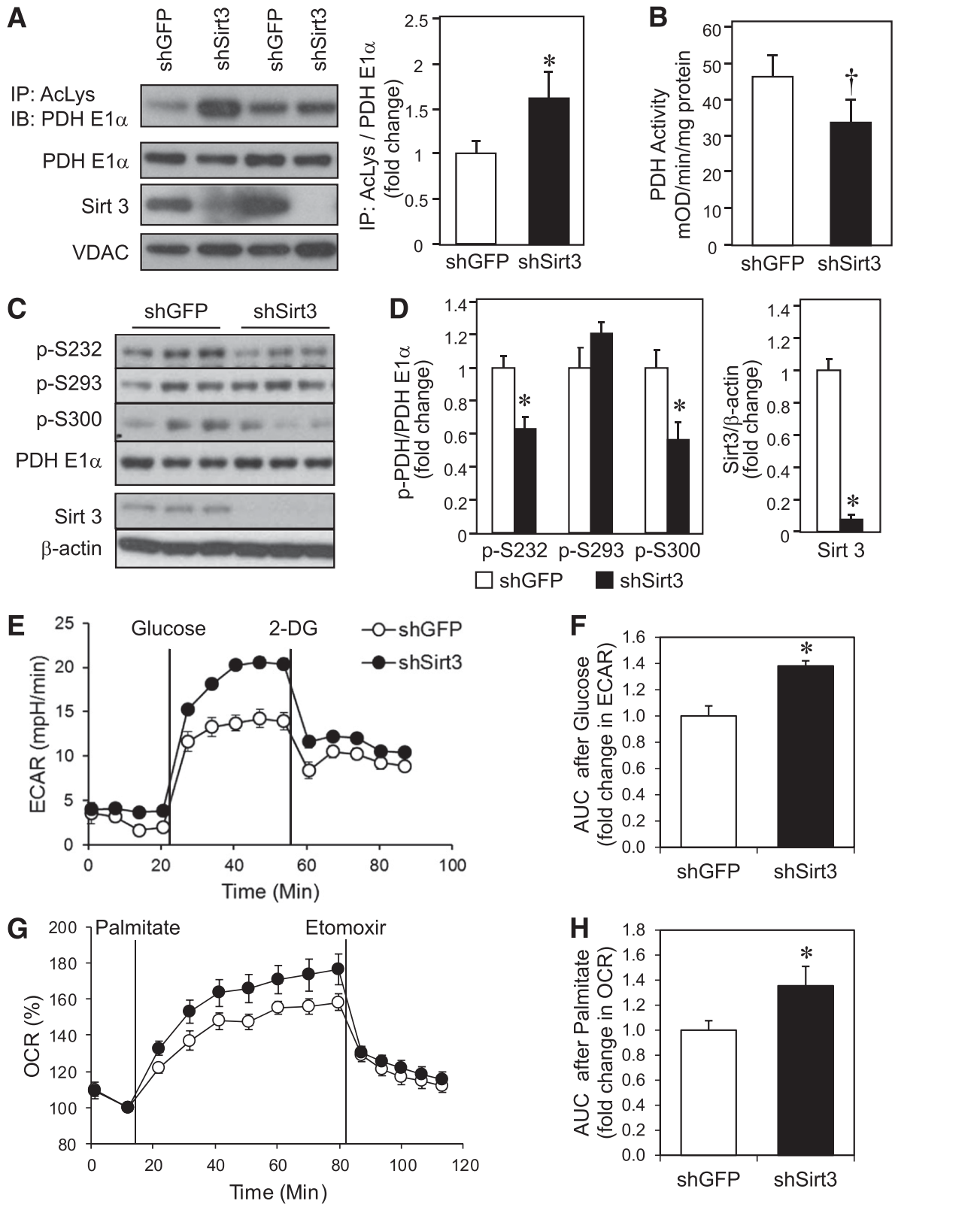

FIG. 5. Sirt3 knockdown in C2C12 myoblasts impairs PDH activity despite decreased phosphorylation of PDH E1α and leads to a substrate switch toward fatty acid utilization. *A*: Total mitochondrial protein lysates from shGFP control and shSirt3 myoblasts were immunoprecipitated (IP) with AcK (AcLys) antibody and subjected to Western blot analysis (IB) using an anti–PDH E1α antibody. The same mitochondrial lysates were directly subjected to Western blot analysis using antibodies against PDH E1α, Sirt3, and voltage-dependent anion channel (VDAC) as a mitochondrial loading control. Densitometry of PDH E1α from AcK immunoprecipitates was normalized to total PDH E1α ($n = 4$ separate experiments; *$P < 0.05$, Student t test). *B*: Total PDH activity was assessed in confluent control and shSirt3 myoblasts using PDH activity microplate assay kit and normalized to total protein from detergent extraction ($n = 5$ separate experiments; †$P < 0.05$, paired t test). *C*: Phosphorylation of PDH E1α and total Sirt3 levels were determined by Western blot analysis of whole cell lysates from confluent shGFP and shSirt3 C2C12 myoblasts. *D*: Densitometry of Western blots from *C* ($n = 3$ separate experiments, *$P < 0.05$, Student t test). *E*: ECAR was measured in shSirt3 and control myoblasts using a Seahorse flux analyzer after incubation in glucose-free Seahorse running media for 1 h at 37°C. A representative tracing of basal and

In the current study, we find that Sirt3 is an important mitochondrial factor in the regulation of skeletal muscle metabolic flexibility by targeting the enzymatic deacetylation of PDH E1α. Thus, when nutrients are abundant, Sirt3 deacetylation promotes PDH activity and postprandial glucose metabolism (Fig. 7*A*). During fasting, there is a decrease of Sirt3 in skeletal muscle, which leads to hyperacetylation of PDH E1α and promotes a metabolic switch from glucose to fatty acids as a predominant substrate (Fig. 7*B*). This can be mimicked by Sirt3 deletion, which results in decreased catalytic activity of PDH, decreased glucose oxidation, and an accumulation of pyruvate and lactate levels even in the fed state. Impaired glucose utilization in Sirt3 KO muscle induces a reliance on fatty acid β-oxidation for energy production. This results in increased breakdown of acylcarnitines and ROS generation and over time leads to insulin resistance (30).

Previous reports have suggested that 24 h of fasting increases Sirt3 levels in muscle (27), but in our hands, 24 h of fasting leads to a consistent decrease in Sirt3 in each muscle group tested. The difference between these two observations may be explained by the timing of the study (mice were killed at 6 P.M. in the former study and at 9 A.M. in our study) and the duration of fasting in the different fed and fasted groups. Peak feeding in mice occurs at the beginning of the nocturnal phase. Thus, fed mice killed at 9:00 A.M. are only a few hours after peak feeding time. On the other hand, when mice are killed at 6:00 P.M., even the "fed" mice are likely to have fasted or partially fasted for as many as 10–12 h prior to study, and the "24-h fasted" mice may have gone without food for as long as 36 h, resulting in dramatic wasting and changes in muscle protein composition (46). Alternatively, there may be circadian changes in expression of Sirt3 or some of its regulators, which is altered during prolonged periods of fasting.

Metabolic flexibility is the ability of an organism to adapt fuel oxidation in response to fuel availability (47). In both insulin resistance and type 2 diabetes, this metabolic flexibility is compromised in that skeletal muscle fails to switch substrate utilization from lipid metabolism to insulin-stimulated glucose oxidation (5,48). The current study demonstrates that mitochondrial Sirt3 can help optimize the switch of substrate oxidation toward glucose utilization by deacetylating PDH, a vital enzyme complex in glucose oxidation. Acute regulation of metabolic flexibility by Sirt3 upon refeeding is not due changes in Sirt3 levels, since 16 h of refeeding is required for full recovery of mRNA and protein levels. These acute changes in substrate flexibility going from the fed to the fasted state are more likely coordinated by a complex network of signaling cascades including insulin and nutrient-dependent phosphorylation events. This acute regulation may still be affected by Sirt3 intracellular partitioning or possible posttranslational modification affecting its deacetylase activity. However, our data support the conclusion that Sirt3 plays an important role in regulating muscle metabolic flexibility upon refeeding by deacetylating PDH and, with dephosphorylation, allows for maximal enzyme activity for glucose oxidation.

Another interesting aspect of Sirt3 physiology is the differential regulation and physiological effects of this enzyme in different tissues. For example, during fasting Sirt3 expression is decreased in muscle but increased in liver (25,30). Mitochondrial protein acetylation patterns confirm that Sirt3 is more active in the fed state in skeletal muscle, whereas in liver Sirt3 is more active during fasting. Sirt3 also has different tissue-specific metabolic effects. Sirt3 deletion in liver suppresses lipid oxidation via suppression of LCAD activity (25), whereas deletion of Sirt3 in muscle decreases glucose oxidation and increases lipid oxidation, at least in part to compensate for PDH inhibition. This dichotomous role of Sirt3 in muscle versus liver may help to explain the report showing minimal changes in global metabolism when Sirt3 is deleted in a tissue-specific manor (49). Muscle-specific deletion of Sirt3 may lead to changes in mitochondrial substrate choice, which are compensated for by opposing Sirt3 action in liver, resulting in a balance at the whole-body level. Nonetheless, this differential regulation of Sirt3 expression and function in a tissue-dependent manner would allow Sirt3 to coordinately regulate divergent pathways of substrate utilization in different organs based on nutrient availability.

Reversible phosphorylation of PDH E1α by PDH kinases inhibits enzyme activity and, in starvation and diabetes, levels of PDH kinases increase in skeletal muscle (14,16,50). PDH kinases can be activated by a decrease in the NAD^+-to-NADH ratio, providing feedback inactivation of the PDH complex (51). Our studies demonstrate that increased acetylation of PDH E1α is associated with decreased PDH complex activity, leading us to speculate that PDH acetylation also regulates complex activity. Indeed, PDH activity was decreased in both Sirt3 KO muscle in vivo and Sirt3 knockdown myoblasts in vitro; the former was associated with increased phosphorylation of Ser^{232} and Ser^{300}, whereas the latter was associated with decreased serine phosphorylation. However, the degree of PDH activity decrease is different in the two models—55–70% in Sirt3 KO in vivo compared with 27% in shSirt3 in vitro—which could be related to phosphorylation status. Lastly, the observation that incubation of Sirt3 KO muscle homogenate in the absence of deacetylase inhibitors partially restored PDH activity supports the notion that acetylation of PDH inhibits its activity. Regulation of enzyme activity by acetylation may also help explain the observed accumulation of α-KG, as α-KG dehydrogenase is similar in structure and regulation to PDH, in that both use an E1 component that may be a target for acetylation and Sirt3-catalyzed deacetylation. Other mechanisms may also contribute to changes in PDH activity. For example, PDH and α-KG dehydrogenase contain many thiol groups, which are sensitive to ROS, and we have previously shown that deletion of Sirt3 causes increased ROS production in muscle from 24-week-old animals (30).

Mass spectrometry–based analysis revealed that PDH E1α is acetylated on multiple lysine residues. We focused our attention on lysine 336, since it exhibited one of the greatest levels of differential acetylation in Sirt3-depleted skeletal muscle. Our attempts to determine whether acetylation at

glucose-stimulated ECARs recorded before and after addition of 25 mmol/L glucose (final concentration) is shown. At the end of the glucose metabolism period, 2-deoxyglucose was injected to give a final concentration of 25 mmol/L. *F*: AUC calculation of glucose-stimulated ECAR from *E*. *G*: A representative tracing of palmitate OCR measured in control and Sirt3 knockdown cells after incubation with substrate-free buffer for 1 h at 37°C. Basal and palmitate-BSA–stimulated OCRs were recorded and plotted as a percentage over basal OCR. Finally, 50 μmol/L etomoxir was injected. *H*: AUC of palmitate-stimulated OCR from *G* ($n = 3$; *$P < 0.05$, Student *t* test). mOD, milli optical density.

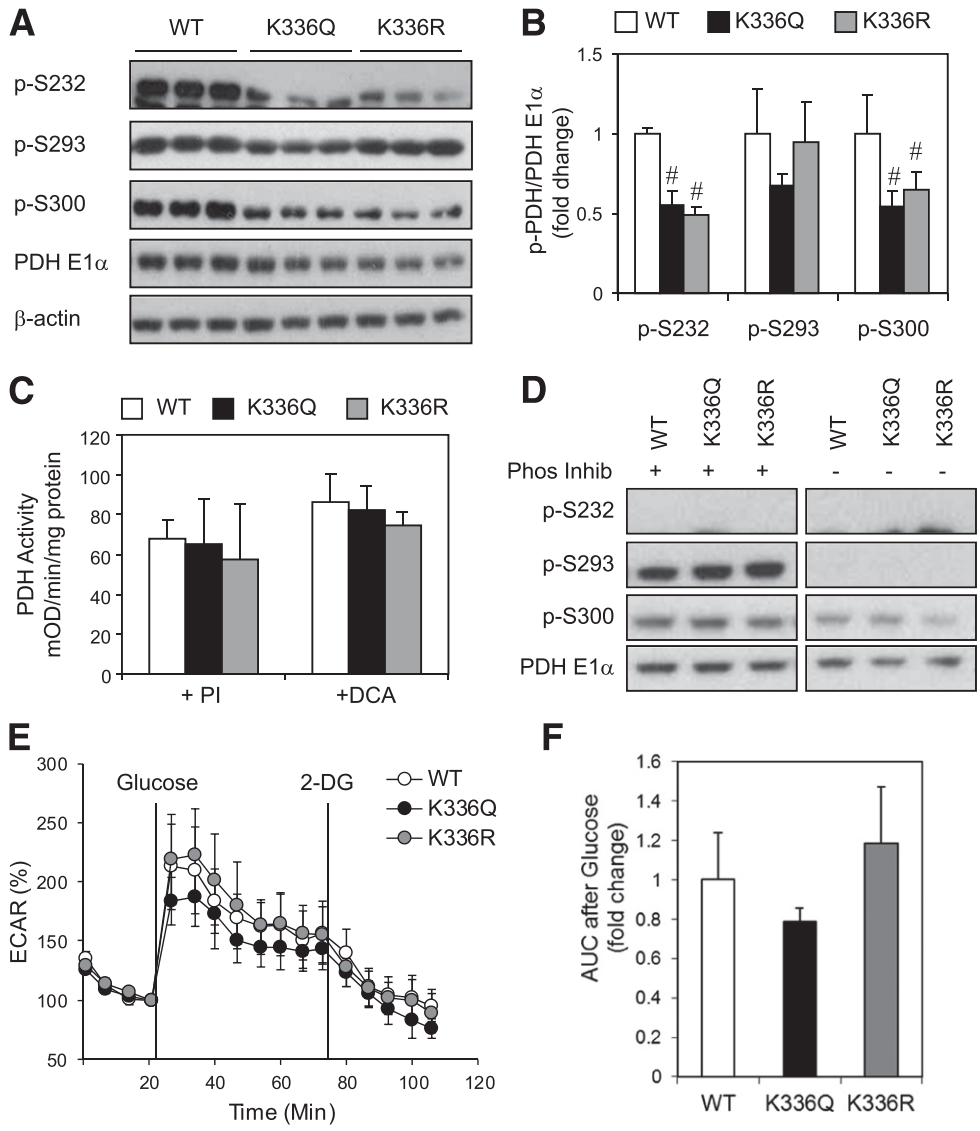

FIG. 6. Expression of a K336Q and K336R mutant of PDH E1α in C2C12 myoblasts decreases phosphorylation but does not affect PDH activity. *A*: Phosphorylation of PDH E1α levels determined by Western blot analysis of whole cell lysates from confluent C2C12 myoblasts expressing WT PDH E1α, K336Q, or K336R mutant of PDH E1α. *B*: Densitometry of Western blots from *A* (n = 3 separate experiments, #$P < 0.05$, ANOVA). *C*: Total PDH activity was assessed in confluent WT, K336Q, or K336R myoblasts using detergent extracts either with PIs 2 and 3 (Sigma) or 20 mmol/L DCA added to the PDH activity assay as described in RESEARCH DESIGN AND METHODS (n = 2–4 separate experiments). *D*: Western blot analysis of detergent extracts from *C* either with PI (Phos Inhib) or with DCA after 3 h incubation at room temperature in buffer 1 of the PDH activity assay kit. *E*: A representative example of Seahorse analysis of glucose-induced ECAR with PDH E1α WT, K336Q, and K336R mutants. *F*: AUC quantification after addition of glucose showed no statistical difference between mutants (n = 4 separate experiments). 2-DG, 2-deoxyglucose.

lysine 336 alone could alter PDH activity using the K336Q (which is regarded as an acetylation mimic) and K336R (which is regarded as a deacetylation mimic) mutations demonstrated that changing the ability of this lysine to become acetylated can cause alterations in phosphorylation of PDH E1α but did not change catalytic function or substrate metabolism in vitro. It is likely that acetylation of other lysine residues in the PDH complex contribute to the observed changes in PDH activity.

Identifying a role of Sirt3 in regulating metabolic flexibility and PDH activity in muscle may provide a new target for preventing and treating metabolic syndrome. Evidence for Sirt3 impacting human metabolic disease is accumulating. We have recently identified a single nucleotide polymorphism in the human Sirt3 gene that decreases its activity and is associated with metabolic syndrome (29). Indeed, targeting PDH activity in muscle for the treatment of diabetes has been proposed as a way to increase glucose disposal, thereby decreasing circulating glucose levels (15). However, many of these treatments induce fasting hypoglycemia as a result of PDH activation during fasting. Since Sirt3 levels decrease in muscle with fasting, pharmacologic activation of Sirt3 in muscle should be beneficial, as it would have maximal effect in the fed state, when glucose levels are highest in diabetes.

In summary, our study demonstrates that Sirt3 plays an important role in control of substrate metabolism and adds another layer of regulation to the multiple pathways that control metabolic flexibility in skeletal muscle. In the fed state, Sirt3 expression/activity in muscle is high, resulting in deacetylation of many mitochondrial proteins, including PDH E1α. This enhances PDH complex activity and postprandial glucose metabolism. Thus, Sirt3 helps orchestrate the efficient use of available nutrients in skeletal muscle by

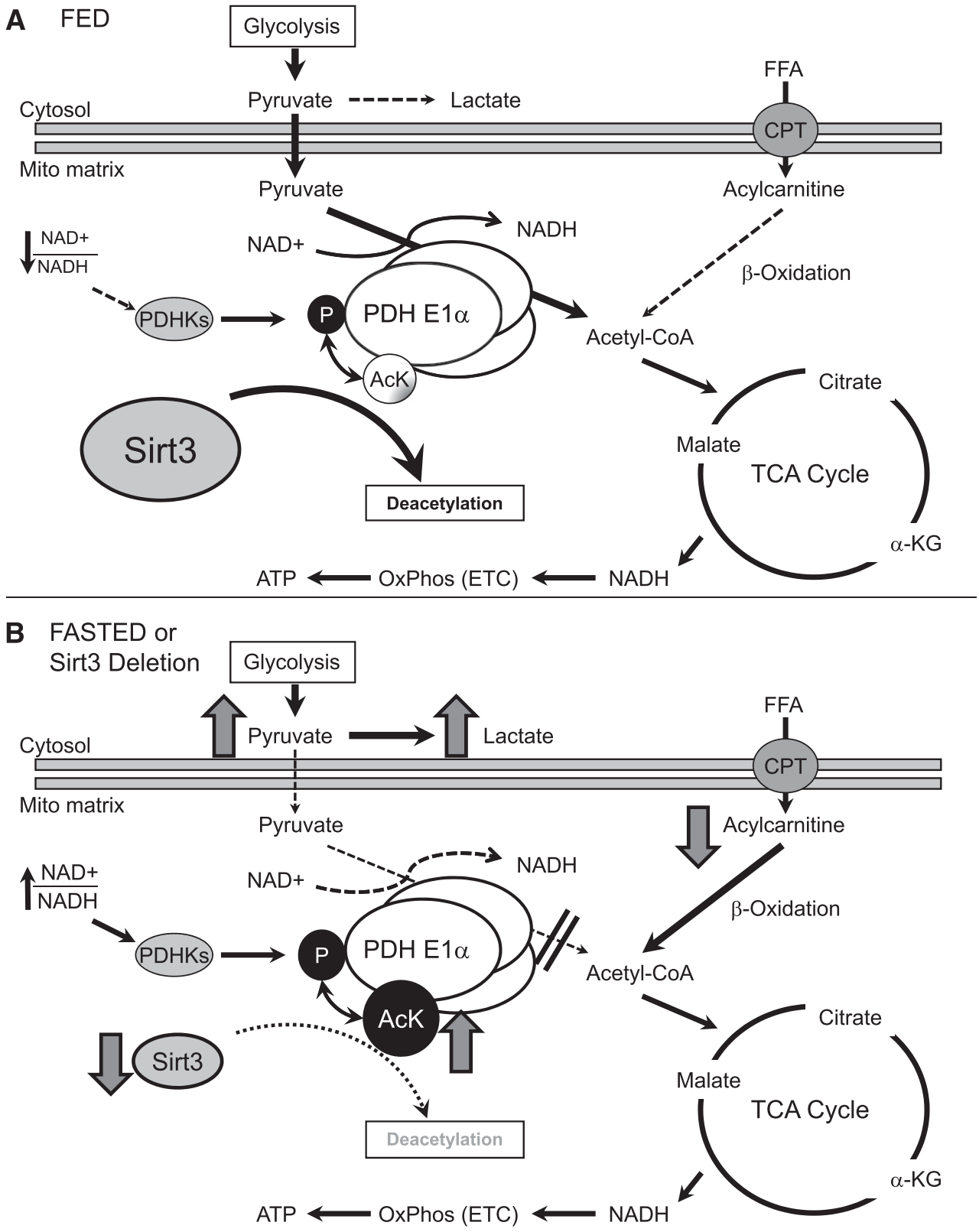

FIG. 7. Model for the role of Sirt3 in control of skeletal muscle substrate metabolism. Sirt3 regulates PDH E1α subunit deacetylation and activates PDH activity. *A*: In the fed state, Sirt3 skeletal muscle expression is abundant and leads to deacetylation of PDH E1α. This is associated with dephosphorylation of PDH allowing for maximal enzyme activation, enhanced glucose utilization, and increased flux of pyruvate to acetyl-CoA used by the tricarboxylic acid (TCA) cycle and electron transport chain (ETC) to generate ATP. *B*: In contrast, decreased Sirt3 expression in muscle by fasting or genetic deletion leads to PDH E1α hyperacetylation and decreased PDH complex activity, which is correlated with increased PDH E1α phosphorylation in vivo. The activity of PDH controls the substrate influx to the TCA cycle from glycolysis. In the case of Sirt3 deletion, inactivation of the PDH caused by hyperacetylation leads to metabolic inflexibility as evidenced by an inability to fully oxidize glucose, a shunt of excess pyruvate toward lactate production, and increased lipid oxidation even in the fed state. CPT, carnitine palmitoyl transferase; FFA, free fatty acid; Mito, mitochondrial; OxPhos, oxidative phosphorylation.

promoting metabolic flexibility through enzymatic deacetylation of PDH. Modulation of mitochondrial acetylation may offer a new therapeutic target for correcting some of the metabolic defects of obesity and type 2 diabetes.

ACKNOWLEDGMENTS

The primary funding for this project was National Institutes of Health Grant R24 DK085610. B.T.O. was funded by Joslin Training Grant T32DK007260. A.K. was funded by German Research Foundation project KL2399/1-1. S.U. was supported by a Human Frontier Science Program Long-Term fellowship. The authors acknowledge the support of National Center for Research Resources shared instrumentation grant S10 RR024615 (to B.W.G.) for the QSTAR Elite mass spectrometer used in these studies.

No potential conflicts of interest relevant to this article were reported.

E.J. and B.T.O. researched data and wrote the manuscript. M.J.R. researched data. A.K. contributed to discussion and researched data. O.R.I., S.U., J.R.B., and K.Y.L. researched data. E.M.V., C.B.N., and B.W.G. researched data and provided materials. C.R.K. oversaw the project, contributed to discussion, and helped write the manuscript. C.R.K. is the guarantor of this work and, as such, had full access to all the data in the study and takes responsibility for the integrity of the data and the accuracy of the data analysis.

REFERENCES

1. Kim JK, Zisman A, Fillmore JJ, et al. Glucose toxicity and the development of diabetes in mice with muscle-specific inactivation of GLUT4. J Clin Invest 2001;108:153–160
2. Fueger PT, Hess HS, Bracy DP, et al. Regulation of insulin-stimulated muscle glucose uptake in the conscious mouse: role of glucose transport is dependent on glucose phosphorylation capacity. Endocrinology 2004;145:4912–4916
3. Storlien L, Oakes ND, Kelley DE. Metabolic flexibility. Proc Nutr Soc 2004;63:363–368
4. van Loon LJ. Use of intramuscular triacylglycerol as a substrate source during exercise in humans. J Appl Physiol 2004;97:1170–1187
5. Befroy DE, Petersen KF, Dufour S, et al. Impaired mitochondrial substrate oxidation in muscle of insulin-resistant offspring of type 2 diabetic patients. Diabetes 2007;56:1376–1381
6. Leone TC, Lehman JJ, Finck BN, et al. PGC-1alpha deficiency causes multisystem energy metabolic derangements: muscle dysfunction, abnormal weight control and hepatic steatosis. PLoS Biol 2005;3:e101
7. Chow L, From A, Seaquist E. Skeletal muscle insulin resistance: the interplay of local lipid excess and mitochondrial dysfunction. Metabolism 2010;59:70–85
8. Espinoza DO, Boros LG, Crunkhorn S, Gami H, Patti ME. Dual modulation of both lipid oxidation and synthesis by peroxisome proliferator-activated receptor-gamma coactivator-1alpha and -1beta in cultured myotubes. FASEB J 2010;24:1003–1014
9. Finck BN, Bernal-Mizrachi C, Han DH, et al. A potential link between muscle peroxisome proliferator- activated receptor-alpha signaling and obesity-related diabetes. Cell Metab 2005;1:133–144
10. Summermatter S, Baum O, Santos G, Hoppeler H, Handschin C. Peroxisome proliferator-activated receptor gamma coactivator 1alpha (PGC-1alpha) promotes skeletal muscle lipid refueling in vivo by activating de novo lipogenesis and the pentose phosphate pathway. J Biol Chem 2010;285:32793–32800
11. Baar K, Song Z, Semenkovich CF, et al. Skeletal muscle overexpression of nuclear respiratory factor 1 increases glucose transport capacity. FASEB J 2003;17:1666–1673
12. Rahman S, Blok RB, Dahl HH, et al. Leigh syndrome: clinical features and biochemical and DNA abnormalities. Ann Neurol 1996;39:343–351
13. Cameron JM, Levandovskiy V, Mackay N, Tein I, Robinson BH. Deficiency of pyruvate dehydrogenase caused by novel and known mutations in the E1alpha subunit. Am J Med Genet A 2004;131:59–66
14. Bowker-Kinley MM, Davis WI, Wu P, Harris RA, Popov KM. Evidence for existence of tissue-specific regulation of the mammalian pyruvate dehydrogenase complex. Biochem J 1998;329:191–196
15. Mayers RM, Leighton B, Kilgour E. PDH kinase inhibitors: a novel therapy for Type II diabetes? Biochem Soc Trans 2005;33:367–370
16. Wu P, Inskeep K, Bowker-Kinley MM, Popov KM, Harris RA. Mechanism responsible for inactivation of skeletal muscle pyruvate dehydrogenase complex in starvation and diabetes. Diabetes 1999;48:1593–1599
17. Zhao S, Xu W, Jiang W, et al. Regulation of cellular metabolism by protein lysine acetylation. Science 2010;327:1000–1004
18. Choudhary C, Kumar C, Gnad F, et al. Lysine acetylation targets protein complexes and co-regulates major cellular functions. Science 2009;325:834–840
19. Schwer B, Eckersdorff M, Li Y, et al. Calorie restriction alters mitochondrial protein acetylation. Aging Cell 2009;8:604–606
20. Michan S, Sinclair D. Sirtuins in mammals: insights into their biological function. Biochem J 2007;404:1–13
21. Milne JC, Denu JM. The Sirtuin family: therapeutic targets to treat diseases of aging. Curr Opin Chem Biol 2008;12:11–17
22. Cooper HM, Spelbrink JN. The human SIRT3 protein deacetylase is exclusively mitochondrial. Biochem J 2008;411:279–285
23. Lombard DB, Alt FW, Cheng HL, et al. Mammalian Sir2 homolog SIRT3 regulates global mitochondrial lysine acetylation. Mol Cell Biol 2007;27:8807–8814
24. Ahn BH, Kim HS, Song S, et al. A role for the mitochondrial deacetylase Sirt3 in regulating energy homeostasis. Proc Natl Acad Sci USA 2008;105:14447–14452
25. Hirschey MD, Shimazu T, Goetzman E, et al. SIRT3 regulates mitochondrial fatty-acid oxidation by reversible enzyme deacetylation. Nature 2010;464:121–125
26. Qiu X, Brown K, Hirschey MD, Verdin E, Chen D. Calorie restriction reduces oxidative stress by SIRT3-mediated SOD2 activation. Cell Metab 2010;12:662–667
27. Palacios OM, Carmona JJ, Michan S, et al. Diet and exercise signals regulate SIRT3 and activate AMPK and PGC-1alpha in skeletal muscle. Aging (Albany, NY Online) 2009;1:771–783
28. Hokari F, Kawasaki E, Sakai A, Koshinaka K, Sakuma K, Kawanaka K. Muscle contractile activity regulates Sirt3 protein expression in rat skeletal muscles. J Appl Physiol 2010;109:332–340
29. Hirschey MD, Shimazu T, Jing E, et al. SIRT3 deficiency and mitochondrial protein hyperacetylation accelerate the development of the metabolic syndrome. Mol Cell 2011;44:177–190
30. Jing E, Emanuelli B, Hirschey MD, et al. Sirtuin-3 (Sirt3) regulates skeletal muscle metabolism and insulin signaling via altered mitochondrial oxidation and reactive oxygen species production. Proc Natl Acad Sci USA 2011;108:14608–14613
31. Chen Y, Zhang J, Lin Y, et al. Tumour suppressor SIRT3 deacetylates and activates manganese superoxide dismutase to scavenge ROS. EMBO Rep 2011;12:534–541
32. Jeoung NH, Wu P, Joshi MA, et al. Role of pyruvate dehydrogenase kinase isoenzyme 4 (PDHK4) in glucose homoeostasis during starvation. Biochem J 2006;397:417–425
33. McKeel DW, Jarett L. Preparation and characterization of a plasma membrane fraction from isolated fat cells. J Cell Biol 1970;44:417–432
34. Schilling B, Rardin MJ, MacLean BX, et al. Platform-independent and label-free quantitation of proteomic data using MS1 extracted ion chromatograms in skyline: application to protein acetylation and phosphorylation. Mol Cell Proteomics 2012;11:202–214
35. Frezza C, Cipolat S, Scorrano L. Organelle isolation: functional mitochondria from mouse liver, muscle and cultured fibroblasts. Nat Protoc 2007;2:287–295
36. Kerr D, Grahame G, Nakouzi G. Assays of pyruvate dehydrogenase complex and pyruvate carboxylase activity. Methods Mol Biol 2012;837:93–119
37. Goodyear LJ, Giorgino F, Balon TW, Condorelli G, Smith RJ. Effects of contractile activity on tyrosine phosphoproteins and PI 3-kinase activity in rat skeletal muscle. Am J Physiol 1995;268:E987–E995
38. Bouskila M, Hirshman MF, Jensen J, Goodyear LJ, Sakamoto K. Insulin promotes glycogen synthesis in the absence of GSK3 phosphorylation in skeletal muscle. Am J Physiol Endocrinol Metab 2008;294:E28–E35
39. An J, Muoio DM, Shiota M, et al. Hepatic expression of malonyl-CoA decarboxylase reverses muscle, liver and whole-animal insulin resistance. Nat Med 2004;10:268–274
40. Wu JY, Kao HJ, Li SC, et al. ENU mutagenesis identifies mice with mitochondrial branched-chain aminotransferase deficiency resembling human maple syrup urine disease. J Clin Invest 2004;113:434–440
41. Jensen MV, Joseph JW, Ilkayeva O, et al. Compensatory responses to pyruvate carboxylase suppression in islet beta-cells. Preservation of glucose-stimulated insulin secretion. J Biol Chem 2006;281:22342–22351

42. Rardin MJ, Wiley SE, Naviaux RK, Murphy AN, Dixon JE. Monitoring phosphorylation of the pyruvate dehydrogenase complex. Anal Biochem 2009;389:157–164
43. Akhmedov D, De Marchi U, Wollheim CB, Wiederkehr A. Pyruvate dehydrogenase E1α phosphorylation is induced by glucose but does not control metabolism-secretion coupling in INS-1E clonal β-cells. Biochim Biophys Acta 2012;1823:1815–1824
44. Bell EL, Emerling BM, Ricoult SJ, Guarente L. SirT3 suppresses hypoxia inducible factor 1α and tumor growth by inhibiting mitochondrial ROS production. Oncogene 2011;30:2986–2996
45. Yang H, Yang T, Baur JA, et al. Nutrient-sensitive mitochondrial NAD+ levels dictate cell survival. Cell 2007;130:1095–1107
46. Jagoe RT, Lecker SH, Gomes M, Goldberg AL. Patterns of gene expression in atrophying skeletal muscles: response to food deprivation. FASEB J 2002;16:1697–1712
47. Galgani JE, Moro C, Ravussin E. Metabolic flexibility and insulin resistance. Am J Physiol Endocrinol Metab 2008;295:E1009–E1017
48. DeFronzo RA, Tripathy D. Skeletal muscle insulin resistance is the primary defect in type 2 diabetes. Diabetes Care 2009;32(Suppl. 2): S157–S163
49. Fernandez-Marcos PJ, Jeninga EH, Canto C, et al. Muscle or liver-specific Sirt3 deficiency induces hyperacetylation of mitochondrial proteins without affecting global metabolic homeostasis. Sci Rep 2012;2:425
50. Linn TC, Pettit FH, Reed LJ. Alpha-keto acid dehydrogenase complexes. X. Regulation of the activity of the pyruvate dehydrogenase complex from beef kidney mitochondria by phosphorylation and dephosphorylation. Proc Natl Acad Sci USA 1969;62:234–241
51. Harris RA, Bowker-Kinley MM, Huang B, Wu P. Regulation of the activity of the pyruvate dehydrogenase complex. Adv Enzyme Regul 2002;42: 249–259